LAWRENCE
LIVERMORE
NATIONAL
LABORATORY

LLNL-JRNL-642514

Precision measurement of the electromagnetic dipole strengths in 11Be

E. Kwan, C. Y. Wu, N. C. Summers, G. Hackman, T. E. Drake, C. Andreoiu, R. Ashley, G. C. Ball, P. C. Bender, A. J. Boston, H. C. Boston, A. Chester, A. Close, D. Cline, D. S. Cross, R. Dunlop, A. Finlay, A. B. Garnsworthy, A. B. Hayes, A. T. Laffoley, T. Nano, P. Navratil, C. J. Pearson, J. Pore, S. Quaglioni, K. Starosta, I. J. Thompson, P. Voss, S. J. Williams, Z. M. Wang

August 20, 2013

Physics Letters B

Disclaimer

Precision measurement of the electromagnetic dipole strengths in ^{11}Be

E. Kwan,[1,*] C. Y. Wu,[1] N. C. Summers,[1] G. Hackman,[2] T. E. Drake,[3] C. Andreoiu,[4] R. Ashley,[4] G. C. Ball,[2] P. C. Bender,[2] A. J. Boston,[5] H. C. Boston,[5] A. Chester,[4] A. Close,[2] D. Cline,[6] D. S. Cross,[4] R. Dunlop,[7] A. Finlay,[7] A. B. Garnsworthy,[2] A. B. Hayes,[6] A. T. Laffoley,[7] T. Nano,[8] P. Navrátil,[2] C. J. Pearson,[2] J. Pore,[4] S. Quaglioni,[1] K. Starosta,[4] I. J. Thompson,[1] P. Voss,[4] S. J. Williams,[2,*] and Z. M. Wang[4,2]

[1]*Lawrence Livermore National Laboratory, PO Box 808, Livermore, CA 94550, USA*
[2]*TRIUMF, 4004 Wesbrook Mall, Vancouver, British Columbia, V6T 2A3 Canada*
[3]*Department of Physics, University of Toronto, Toronto, Ontario, M5S 1A7, Canada*
[4]*Department of Chemistry, Simon Fraser University, Burnaby, British Columbia, V5A 1S6 Canada*
[5]*Department of Physics, University of Liverpool, Liverpool L69 7ZE, United Kingdom*
[6]*Department of Physics & Astronomy, University of Rochester, Rochester, NY, 14627, USA*
[7]*Department of Physics, University of Guelph, Guelph, Ontario, N1G 2W1 Canada*
[8]*University of Windsor, Windsor Ontario, N9B 3P4 Canada*

(Dated: August 20, 2013)

The electromagnetic dipole strength in ^{11}Be between the bound states has been measured using low-energy projectile Coulomb excitation at bombarding energies of 1.73 and 2.09 MeV/nucleon on a ^{196}Pt target. An electric dipole transition probability $B(E1; 1/2^- \rightarrow 1/2^+) = 0.102(2)\ e^2\text{fm}^2$ was determined using the semi-classical code Gosia, and a value of 0.098(4) $e^2\text{fm}^2$ was determined using the Extended Continuum Discretized Coupled Channels method with the quantum mechanical code FRESCO. These extracted *B(E1)* values are consistent with the average value determined by a model-dependent analysis of intermediate energy Coulomb excitation measurements and are approximately 14% lower than that determined by a lifetime measurement. The much-improved precision in the measured *B(E1)* values will help in our understanding of and better improve the realistic inter-nucleon interactions.

PACS numbers: 27.20.+n,25.70.De,25.60.-t

Nuclei far from the line of β-stability have garnered much interest because phenomena, different from those observed near stability, are known to occur such as the reordering of the shells leading to the quenching of the magic numbers at $N = 8$ and 20 [1, 2]. In very light nuclei in the vicinity of the neutron drip line, loosely bound systems with extended wave functions known as halo nuclei have been observed [3]. For example, the ground state of the one-neutron halo nucleus ^{11}Be is not characterized by a neutron in a $p_{1/2}$ shell, but arises due to an intruder state from the sd shell [4]. In this region of the chart of nuclides, nuclei contain relatively few nucleons and can be described by means of first principle (or *ab initio*) calculations using accurate microscopic Hamiltonians. In addition, due to the highly clustered nature of the low-lying states, the ^{11}Be nucleus is described well by a two-body cluster model in which a deformed ^{10}Be core is coupled to the neutron [5]. Using such few-body models, cross sections can be calculated using the quantum mechanical code FRESCO [6], which now implements the Extended Coupled Discretized Continuum Channels (XCDCC) method [7] in order to include the ^{11}Be model of Ref. [5].

The ^{11}Be nucleus represents one of the best examples of parity inversion of the ground state and disappearance of the $N = 8$ shell closure with increasing neutron-to-proton ratio. Due to the asymptotic behavior of the wave function, large-scale bound-state calculations using realistic nucleon-nucleon interactions within the *ab initio* No-Core Shell Model (NCSM) were shown to have difficulty reproducing the correct parity sequence of the ground and first excited states of this halo nucleus [8]. Using a microscopic cluster technique known as the resonating-group method combined with the no-core shell model (NCSM/RGM), it was demonstrated in Refs. [9, 10] that the proper treatment of the continuum is critical to lower the energy of the first $1/2^+$ state, which is dominated by the S-wave neutron-^{10}Be ground state configuration. Even though the correct parities for the bound states were predicted, these NCSM/RGM calculations were restricted to just four states of the ^{10}Be core and used a limited model space for the ^{10}Be wave functions.

The influence of additional excitations of the ^{10}Be core can be addressed within the more complete framework of the no-core shell model with continuum (NCSMC), introduced recently [11, 12]. Preliminary results for ^{11}Be, obtained with soft similarity-renormalization-group [13, 14] evolved chiral NN interactions [15], show that indeed excitations beyond the lowest two excited states in ^{10}Be are needed to reach convergence [16]. At the same time, these calculations indicate that the so far neglected NNN interactions, those induced by the renormalization procedure and those present in the initial chiral Hamiltonian, must be included in the calculations to properly describe the bound states of ^{11}Be as well as its resonances.

Work currently underway to incorporate the NNN force into the NCSMC formalism should lead to the first complete *ab initio* picture of the ^{11}Be nucleus, address-

ing both the role of the ^{10}Be core excitations and the underlying nuclear interactions. The precise measurement of the *B(E1)* between the ^{11}Be bound states as well as of the *B(E1)* strength to the continuum obtained in this experiment will provide a critical test of the quality of chiral nuclear interactions as well as of the NCSMC many-body technique that aims at a unified description of both bound and unbound states.

^{11}Be is interesting experimentally not only because the parities of the ground and the first excited states are inverted, but also because strong electric dipole $E1$ strengths have been observed between the bound states and from the ground state to the continuum in break-up reactions . The reduced transition probability, $B(E1) = 0.116(12)\ e^2\text{fm}^2$ or 0.36 Weisskopf units (W.u.), was derived from the mean lifetime of 166(15) fs deduced from a Doppler shift attenuation measurement (DSAM) [17]. It is the strongest known electric dipole transition between bound states in nuclei. The typical strength of electric dipole transitions observed range from around 10^{-3} to 10^{-6} W.u. This strength is usually suppressed due to incoherent "interference between many single-particle components in the transition density" [18].

The *E1* strength in ^{11}Be was also measured in subsequent Coulomb excitation experiments with accuracies of ∼10% at intermediate energies from 39 to 64 MeV/nucleon [19–22] and has a weighted average value of $0.105(7)e^2\text{fm}^2$ [22], excluding the measurement of Ref. [19]. The analysis of the Coulomb excitation experiments at 60 and 64 MeV/nucleon [20, 21] relied on a semi-classical theory based on a first-order perturbation theory which assumes that the excitation occurs in a single-step process and does not include contributions due to the continuum and higher order effects, such as nuclear absorption and excitation. At these intermediate projectile energies, both Rutherford scattering and relativistic effects are important. A model dependent analysis at projectile energies of 39 and 59 MeV/nucleon [22] using the XCDCC method [7], indicated that the continuum, nuclear and higher order effects will either enhance or suppress the excitation probability by ∼2-20%. The correction due to the nuclear contributions is much larger than the values calculated by previous analyses using an eikonal model on light carbon and beryllium targets [20, 23]. These effects are expected to be minimized by lowering the projectile energy to well below the Coulomb barrier.

Significant $E1$ strength was also observed to the continuum of ^{11}Be in breakup reactions at intermediate energies. This strength to the continuum, which was observed to have an integrated value up to E_x= 4 MeV of $\sim 1\ e^2\text{fm}^2$ and peak at ∼800 keV, amounts to about 4% of the energy-weighted $E1$ sum rule and exhausts 70% of the cluster sum-rule value [24]. The *B(E1)* strength to the continuum of ^{11}Be has been measured to ∼5% accuracy [24–26], but with discrepancies ∼15% between the reported strengths. In part, this may be the result of contributions from the excitation of ^{10}Be not subtracted from the distribution. In addition, calculations of the nuclear contribution to the dissociation of ^{11}Be using the continuum discretized coupled-channels theory found that Coulomb-nuclear interference effects, which can be either constructive or destructive, can not be ignored since it does not simply scale with the geometric size [27]. Improvement to the precision of the *B(E1)* values between the bound states and from the $1/2^+$ ground state (g.s.) to the continuum is necessary to resolve the experimental discrepancies. Furthermore, new precision measurements are necessary to isolate the importance of individual terms of the realistic Hamiltonian included in theories like the *ab initio* NCSM/RGM [9] and will help answer some of the issues outlined earlier.

In this article, we present two high-precision Coulomb excitation measurements of the *B(E1)* strength between the bound 320 keV $1/2^-$ state and g.s. in ^{11}Be using projectile energies well below the Coulomb barrier. The experiments were fielded at TRIUMF's Isotope Separator and Accelerator (ISAC II). The ^{11}Be beams, with intensities of 1-2 × 10^6 ions per second, were produced by the Resonance Ionization Laser Ion Source [28] and then accelerated to 1.73 and 2.09 MeV/nucleon using the radio frequency quadrupole and drift-tube linear accelerators [29]. A 2.92 mg/cm^2 platinum target enriched to 94.57% in ^{196}Pt was used to scatter the ^{11}Be beam into the Bambino Silicon detector array, which was designed and built by the LLNL-Rochester collaboration and consisted of two double-sided segmented 140-μm thick Si detectors. Bambino has been successfully employed in a number of experiments since 2005, which resulted in four publications [30–33]. Gamma rays emitted from the excited nucleus and in coincidence with the charge particles detected by the Bambino array were measured using 12 segmented high purity germanium (HPGe) clover detectors known as the TRIUMF-ISAC Gamma-Ray Escape Suppressed Spectrometer (TIGRESS) [34], which surrounded the Si detectors. Shown in Fig. 1(a) and (b) are the measured γ-ray spectra for the region of interest at incident energies of 2.09 and 1.73 MeV/nucleon, respectively, in the lab (solid curves) and projectile (dashed curves) frames. The transitions from the first excited state to the g.s. in both ^{196}Pt and ^{11}Be are labeled. The two Si detectors, which are each segmented into 32 equal sectors to measure the vertical angle relative to the floor (ϕ) and 24 rings for an angular coverage relative to the beam axis (θ) between [18.6° and 47.0°] and [133.0° and 161.4°] in the lab frame, allowed for an energy resolution of 1.4% full-width at half-max for the 320 keV transition in the Doppler-shift corrected spectra. Gamma-rays events due to scattering in the room, natural activity, and β decay of ^{11}Be within a 125 ns coincidence gate were subtracted out using events outside the acceptance window corresponding to random background.

The γ-ray yields were examined at ten angular regions, six at forward angles and four at backward angles with $1.2-5.1\%$ statistical errors. The γ-ray yields in each region from the 320 keV transition in ^{11}Be were normalized by a constant, which was determined relative to the total intensities for the $2^+ \rightarrow 0^+$ transition in ^{196}Pt. Using the adopted value for the $B(E2;2^+ \rightarrow 0^+) = 0.274(1)e^2b^4$ [35] for the 356 keV 2^+ to the 0^+ g.s. transition, the ^{196}Pt yields were calculated using the semi-classical least squares fitting Coulomb excitation code Gosia [36] and the quantum mechanical reaction code FRESCO[6]. Matrix elements for transitions from the second excited 2^+, first two 4^+ states, and first 6^+ state in ^{196}Pt were included to account for the feeding to the 356 keV state. The analysis with Gosia was confined to the forward angles, since the effects of the continuum and the break-up mechanism, which are not included in the semi-classical approximation, were found to be negligible in this region for the 320 keV transition according to a full quantum mechanical calculation using XCDCC. A second analysis using the XCDCC method was implemented to include the continuum on the *B(E1)* strength of the 320 keV transition in ^{11}Be. The extended wave function for ^{11}Be in the XCDCC code was calculated assuming a deformed core + coupled-channels particle cluster model [5] consisting of ^{10}Be plus a neutron. A deformed Woods-Saxon potential was used to describe the interaction between the ^{10}Be core and the neutron. The potential parameters were adjusted to fit the binding energies of the ground and excited states, and to reproduce the *B(E1)* strengths between them [22]. The ^{10}Be + neutron continuum was included using the XCDCC method, with breakup included to s-, p-, and d-waves, and up to approximately 2 MeV in relative energy between the ^{10}Be and neutron.

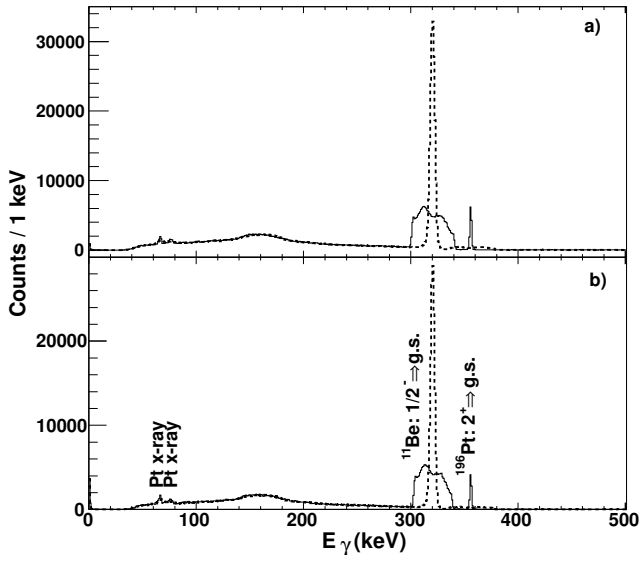

FIG. 1: The summed background subtracted γ spectra at incident energies of (a) 2.09 and (b) 1.73 MeV/nucleon in the lab and projectile frames, the solid and dashed histograms, respectively.

The relative efficiency between the 320 keV ^{11}Be transition and the 356 keV transition in ^{196}Pt for the TIGRESS array with the HPGe detectors configured in its closest geometry of $r = 11$ cm from the center target is 1.07, which was determined using ^{60}Co, ^{133}Ba, and ^{152}Eu calibration sources. All the γ-ray yields for the forward scattering angles are corrected by the measured single events detected by the Si detectors, *i.e.* the Rutherford cross section. The systematic uncertainties in the normalization of the Be yields for both codes at each projectile energy were determined by varying the uncertainty of the $2^+ \rightarrow 0^+$ transition in the ^{196}Pt data until a reduced $\chi^2 \approx 1$ was achieved. This resulted in systematic uncertainties of 5.3% and 7.5% at 1.73 and 2.09 MeV/nucleon, respectively, for the normalization using Gosia and 11% and 18% with XCDCC. The latter has bigger uncertainties because the data from the backward scattering angles are included.

The expected yields at each angular region were then calculated using Gosia and XCDCC for ^{11}Be iteratively using various *B(E1)* strengths and were compared to the measured yields to determine the summed χ^2 distributions at both projectile energies. The adopted *B(E1)* values from the current work obtained from each code and their uncertainties were determined through the χ^2 distribution in accordance to Ref. [37]. In the analysis with Gosia, a $B(E1;1/2^- \rightarrow 1/2^+) = 0.102(2)\ e^2\text{fm}^2$ was deduced for the 320 keV transition to the g.s. This value is consistent with the previous results from Coulomb excitation at intermediate energies, but is about 14% lower than the DSAM value reported in Ref. [17]. In the analysis using the XCDCC code, a $B(E1;1/2^- \rightarrow 1/2^+) = 0.098(4)\ e^2\text{fm}^2$ was determined, which is consistent with the values deduced using Gosia and the previous results of Coulomb excitation at intermediate energies [22]. Shown in Fig. 2 is a comparison of the measured γ yields at 1.73 and 2.09 MeV/nucleons with the calculated yields from Gosia (panel b) and XCDCC (panel a) using our derived *B(E1)* values from each code. The dashed lines represent the expected yields from varying the *B(E1)* strength by one standard deviation. A similar comparison of the measured yields and the calculated ones from XCDCC for the backward angles is plotted in Fig. 3.

The *B(E1)* strength to the continuum was also calculated using the XCDCC code with the same potentials as those used to generate the wave functions for a given *B(E1)* strength between the bound states. An integrated strength of 0.95(3) $e^2\text{fm}^2$ to the continuum up to 4 MeV was estimated based on this *B(E1)* strength between the bound states and is consistent with those reported in Refs. [25, 26]. Variations for the coupling strength to the continuum in ^{11}Be indicated negligible effect on the calculated yields for the 320 keV transition suggesting

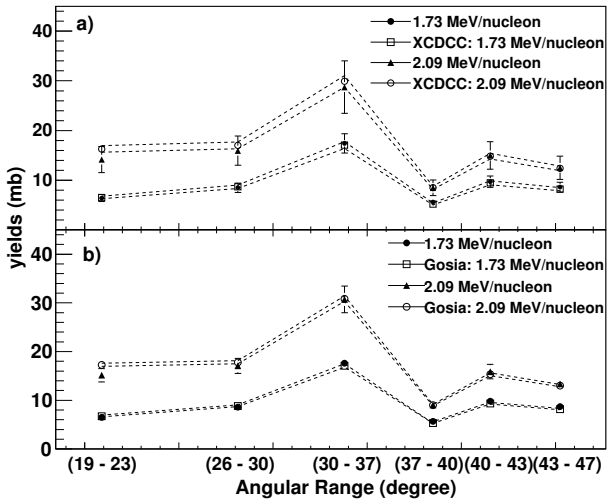

FIG. 2: Comparison of the calculated yields from a) XCDCC with $B(E1) = 0.098\ e^2\text{fm}^2$ and b) Gosia with $B(E1) = 0.102\ e^2\text{fm}^2$ to the experimental values. The dashed lines represent the calculated yields from varying the *B(E1)* values by one standard deviation: 4% in XCDCC and 2% in Gosia.

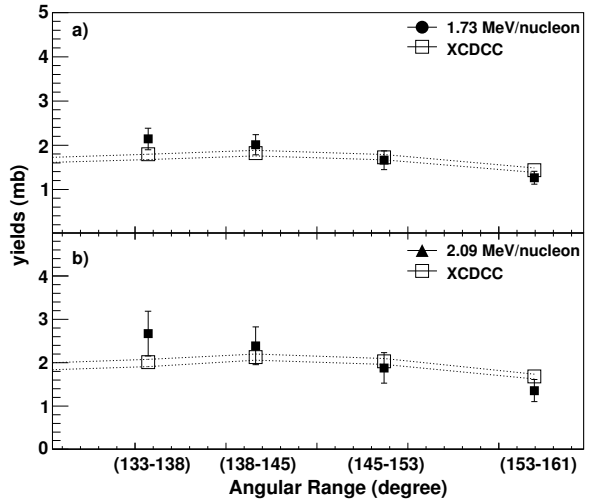

FIG. 3: Comparison of the calculated yields from XCDCC with $B(E1) = 0.098\ e^2\text{fm}^2$ at a) 1.73 MeV/nucleon and b) 2.09 MeV/nucleon to the experimental values in the backward angles. The dashed lines represent the calculated yields from varying the *B(E1)* values by one standard deviation of 4%.

that the ^{11}Be strength to the continuum is insensitive to the current analytical approach.

In summary, a precision measurement of the *E1* strength in one-neutron halo nucleus, ^{11}Be, was carried out using the Coulomb excitation technique. The $B(E1; 1/2^- \rightarrow 1/2^+) = 0.102(2)$ and $0.098(4)\ e^2\text{fm}^2$ values obtained for the transition between the bound states was determined using a semi-classical approach and a quantum mechanical reaction theory, respectively. The current measured value is consistent with the weighted average of the earlier measurements using the intermediate Coulomb excitation technique with a model-dependent analysis. The uncertainty has been improved significantly in the current measurement and will help optimize the parameter selection for different terms in the realistic nucleon-nucleon and three-nucleon interactions.

This work was performed in part under the auspices of the U.S. DOE by LLNL under Contract DE-AC52-07NA27344 and the National Science Foundation. Partially support by the Natural Sciences and Engineering Research Council of Canada is also acknowledge. TRIUMF receives federal funding via a contribution agreement from the National Research Council of Canada.

* Present address: National Superconducting Cyclotron Laboratory, East Lansing, Michigan, 48824, USA

[1] T. Otsuka, et al, Phys. Rev. Lett. **87**, 082502 (2001).
[2] O. Sorlin and M.-G. Porquet, Prog. Part. Nucl. Phys **61**, 602 (2008).
[3] A. Krieger, et al., Phys. Rev. Lett. **108**, 142501 (2012).
[4] W. Geithner, et al., Phys. Rev. Lett. **83**, 3792 (1999).
[5] F. M. Nunes, I. J. Thompson, and R. C. Johnson, Nucl. Phys. A **596**, 171 (1996).
[6] I. J. Thompson, Comput. Phys. Rep. **7**, 167 (1988).
[7] N. C. Summers, F. M. Nunes, and I. J. Thompson, Phys. Rev. C **74**, 014606 (2006).
[8] C. Forssén, P. Navrátil, W. E. Ormand, and E. Caurier, Phys. Rev. C **71**, 044312 (2005).
[9] S. Quaglioni and P. Navráil, Phys. Rev. Lett. **101**, 092501 (2008).
[10] S. Quaglioni and P. Navráil, Phys. Rev. C **79**, 044606 (2009), and references therein.
[11] S. Baroni, P. Navráil, and S. Quaglioni, Phys. Rev. Lett. **110**, 022505 (2013).
[12] S. Baroni, P. Navráil, and S. Quaglioni, Phys. Rev. C **87**, 034326 (2013).
[13] S. K. Bogner, R. J. Furnstahl, and R. J. Perry, Phys. Rev. C **75**, 061001.
[14] R. Roth, S. Reinhardt, and H. Hergert, Phys. Rev. C **77**, 064003 (2008).
[15] D. R. Entem and R. Machleidt, Phys. Rev. C **68**, 041001 (2003).
[16] P. Navrátil, Private communicaton.
[17] D. J. Millener, et al., Phys. Rev. C **28**, 497 (1983).
[18] B. A. Brown, Prog. Part. Nucl. Phys. **47**, 517 (2001).
[19] R. Anne, et al., Z. Phys **352**, 397 (1995).
[20] M. Fauerbach, et al., Phys. Rev. C **56**, R1 (1997).
[21] T. Nakamura, et al., Phys. Lett. B **394**, 11 (1997).
[22] N. C. Summers, et al., Phys. Lett. B **650**, 124 (2007).
[23] T. Glasmacher, in *The Euroschool Lectures on Physics With Exotic Beams Vol. III*, edited by J. S. Al-Khalili and E. Roeckl (Springer, Berlin Heidelberg, 2009) p. 27.
[24] N. Fukuda, et al., Phys. Rev. C **70**, 054606 (2004).
[25] T. Nakamura, et al., Phys. Lett. B **331**, 296 (1994).
[26] R. Palit, et al., Phys. Rev. C **68**, 034318 (2003).
[27] M. S. Hussein, et al., Phys. Lett. B **640**, 91 (2006).
[28] E. J. Prime, et al., Hyperfine Int. **171**, 127 (2006).

[29] R. E. Laxdal, Nucl. Instrum. Methods B **204**, 400 (2003).
[30] M. A. Schumaker, et al., Phys. Rev. C **78**, 044321 (2008).
[31] M. A. Schumaker, et al., Phys. Rev. C **80**, 044325 (2009).
[32] A. M. Hurst, et al., Phys. Lett. B **674**, 168 (2009).
[33] R. Kanungo, et al., Phys. Lett. B **682**, 391 (2010).
[34] H. C. Scraggs, et al., Nucl. Instrum. Methods A **543**, 431 (2005).
[35] X. Haung, Nucl. Data Sheets **108**, 1093 (2007).
[36] T. Czosnyka, D. Cline, and C. Y. Wu, Am. Phys. Soc. **28**, 745 (1983).
[37] D. Cline and P. M. S. Lesser, Nucl. Instrum. Methods **82**, 291 (1970).